

CO₂ reforming of CH₄ over Ni/SBA-15: Influence of Ni-loading methods

H.D. Setiabudi*, N.S.A. Razak, F.R.M. Suhaimi and F.N. Pauzi

Faculty of Chemical and Natural Resources Engineering, Universiti Malaysia Pahang, 26300 Gambang, Kuantan, Pahang, Malaysia.

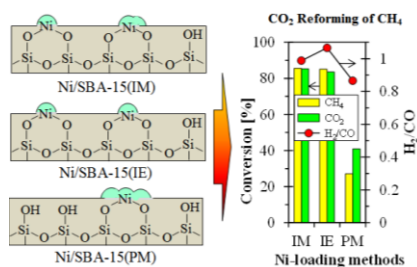
*Corresponding Author: herma@ump.edu.my

Article history :

Received 21 July 2016

Accepted 2 Sept 2016

GRAPHICAL ABSTRACT



ABSTRACT

A series of Ni/SBA-15 catalysts were prepared with three different methods which are impregnation (IM), ion exchange (IE) and physical mixing (PM) for CO₂ reforming of CH₄. The XRD, TEM, BET, FTIR and TGA analyses showed that the quantity of Ni-support interaction (Ni-O-Si) by substitution of the OH with Ni species followed the order of Ni/SBA-15(IE) > Ni/SBA-15(IM) > Ni/SBA-15(PM), while the size of Ni particles, an agglomeration of Ni particles and blockage of the pores increased with the order of Ni/SBA-15(IE) < Ni/SBA-15(IM) < Ni/SBA-15(PM). At temperature studied, the activity of catalysts followed the order of Ni/SBA-15(IE) ≈ Ni/SBA-15(IM) > Ni/SBA-15(PM), while the stability of catalysts followed the order of Ni/SBA-15(IE) > Ni/SBA-15(IM) > Ni/SBA-15(PM). The excellent performance of Ni/SBA-15(IE) was related with the higher formation of Ni-support interaction, which altered the properties of catalyst towards an excellent catalytic performance. Meanwhile, the lowest activity of Ni/SBA-15(PM) was related to the higher agglomeration of Ni particles that were decorating on the surface part of SBA-15 arose from the weaker Ni-support interaction. This study provides new perspectives on the Ni-based catalyst, particularly on the influence of Ni-loading methods on the properties and catalytic performance of Ni/SBA-15 towards CO₂ reforming of CH₄.

Keywords: Ni-loading methods, Ni/SBA-15, Dry reforming, Ni-support interaction

© 2016 Dept. of Chemistry, UTM. All rights reserved
| eISSN 0128-2581 |

1. INTRODUCTION

Climate change has become one of the main concerns of humanity in recent century. The negative effects of greenhouse gasses (GHGs) emission on people's health are unavoidable fact. The radiation from the surface of the earth can be trapped by GHGs in the atmosphere, and global warming is the main concern of GHGs effect [1]. Therefore, there has been an increasing pressure from the public all over the world to control the rising rate of GHGs production in the world. Catalytic reforming of methane (CH₄) with carbon dioxide (CO₂) also known as dry reforming, has recently attracted considerable attention due to the simultaneous utilization and reduction of two GHGs (CH₄ and CO₂), into syngas (H₂ and CO) which is preferred for the synthesis of valuable oxygenated chemicals and log-chain hydrocarbons [2].

The CO₂ reforming of CH₄ has been studied extensively using variety of supported metal catalysts. Among others, catalysts based on noble metals such as Pd, Pt and mainly Rh, have been reported to have good activity and carbon deposition resistance to the reforming reaction [3]. However, Ni has drawn remarkable attention owing to its wider availability and lower cost, which is more practical from an industrial standpoint [4-5]. Apart from the metal, catalyst support is another important parameter in achieving

favourable features of the catalyst. Up to now, various supports have been used in CO₂ reforming of CH₄ including SBA-15 [1-2], MSN [4], alumina [6], ZrO₂ [7], SiO₂ [8] and zeolites [5]. Among others, SBA-15 has been investigated as a potential candidate for the CO₂ reforming of CH₄, owing to its high surface area, excellent thermal stability and good dispersion of Ni particles on SBA-15 [1-2].

It is well known that the methodologies of catalyst preparation have a significant effect on the properties and catalytic performance. Although several studies have reported the effects of Ni-loading methods on the properties of Ni/SBA-15 [2,9], however, there is no publication concerning the influence of Ni-loading methods on the properties and catalytic activity of CO₂ reforming of CH₄ by comparing the methods of impregnation (IM), ion-exchange (IE) and physical mixing (PM). Thus, in this work, we are focusing on the effect of Ni-loading methods (IM, IE and PM) on the properties and catalytic activity of Ni/SBA-15 towards CO₂ reforming of CH₄. The properties of catalysts were analyzed using XRD, TEM, BET, FTIR and TGA analyses. The relationship between the effect of Ni-loading methods and catalytic activity in CO₂ reforming of CH₄ was investigated using microcatalytic reactor.

2. EXPERIMENTAL

2.1 Catalyst Preparation

The SBA-15 was prepared according to the method reported by Zhao et al. [10]. The triblock copolymer P123 (EO₂₀PO₇₀EO₂₀, Aldrich) was used as the structure-directing agent and tetraethyl orthosilicate (TEOS, Merck) as the silica source. The P123 was dissolved in the solution of deionized water and 2M hydrochloric acid solution and stirred at 40 °C for 1 h. The TEOS was slowly added to the mixture with vigorous stirring at 40 °C for 24 h, and the precipitate product was obtained. The precipitate product was filtered, washed with deionized water and dried overnight at 110 °C. The sample was calcined at 550 °C for 3 h to remove the triblock copolymer.

The Ni/SBA-15 catalyst was prepared by three types of preparation methods which were impregnation (IM), ion exchange (IE) and physical mixing (PM). For impregnation method, an appropriate amount of Ni salt precursor, Ni(NO₃)₂·6H₂O (Merck, 99%) was mixed with SBA-15, and then was heated slowly at 80 °C under continuous stirring and maintained at that temperature until nearly all the water had evaporated. The solid residue was dried overnight at 110 °C followed by calcination at 550 °C for 3 h to give dark grey colored Ni/SBA-15(IM). For the ion exchange method, an appropriate amount of Ni salt precursor, Ni(NO₃)₂·6H₂O (Merck, 99%) was mixed with SBA-15 under continuous stirring for 12 h. The product was filtered and dried overnight at 110 °C followed by calcination at 550 °C for 3 h to obtain Ni/SBA-15(IM). For the physical mixing method, an appropriate amount of Ni salt precursor, Ni(NO₃)₂·6H₂O (Merck, 99%) was calcined at 550 °C for 3 h to obtain black NiO powder. A desired amount of NiO was physically mixed with SBA-15 and calcined for 3 h at 550 °C to give a dark grey colored Ni/SBA-15(PM). In this study, Ni loading was adjusted at 5wt% for all catalysts.

2.2 Catalyst Characterization

The crystalline structure of the catalyst was determined by X-ray diffraction (XRD) recorded on powder diffractometer (Philips X' Pert MPD, 3 kW) using a Cu K α radiation ($\lambda = 1.5405\text{\AA}$). The primary crystallite size of NiO (D_{NiO}) was calculated by means of the Scherrer equation [11]:

$$D_{NiO} = \frac{0.9\lambda}{B \cos \theta} \quad (1)$$

where λ is the X-ray wavelength corresponding to Cu-K α radiation (0.15405 nm), B is the broadening (in radians) of the nickel (200) reflection and θ is the angle of diffraction corresponding to peak broadening.

Transmission electron microscopy (TEM) was carried out using a Philips CM12. The sample was dispersed

in acetone by sonication, and deposited on an amorphous, porous carbon grid. The Brunauer-Emmett-Teller (BET) analysis of the catalyst was conducted using AUTOSORB-1 model AS1 MP-LP instrument at 77 K. The Fourier Transform Infrared (FTIR) measurement was carried out using Thermo Nicolet Avatar 370 DTGS model in KBr matrix in order to study the chemical properties of catalysts and to identify the interaction of Ni species with SBA-15. The phenomenon of weight loss, which results from heating the samples were analyzed by Thermogravimetric analysis (TGA) (TGA Q500, TA Instruments) under a mixture of air (20% O₂/80% N₂) with heating rate of 5 °C min⁻¹ up to 900 °C.

2.3 Catalytic Testing

The catalytic CO₂ reforming of CH₄ was conducted in a microcatalytic reactor at atmospheric pressure and reaction temperature of 800 °C. Prior to the reaction, 0.2 g of catalyst was reduced in a H₂ flow of 50 ml/min for 3 h at 700 °C. The feeding gas flow rate to the reactor was set at 50 ml/min, with a ratio of CH₄:CO₂:N₂ = 1:1:1, and N₂ was used as a carrier gas. The effluent gas was analyzed with an Agilent gas chromatography equipped with a thermal conductivity detector (TCD).

The CH₄ and CO₂ conversion were calculated according to the following equations;

$$\text{CO}_2 \text{ Conversion, } X_{CO_2} = \frac{F_{CO_2,in} - F_{CO_2,out}}{F_{CO_2,in}} \times 100\% \quad (2)$$

$$\text{CH}_4 \text{ Conversion, } X_{CH_4} = \frac{F_{CH_4,in} - F_{CH_4,out}}{F_{CH_4,in}} \times 100\% \quad (3)$$

where F is the molar flow rate for particular compound. The product distribution ratio, H₂/CO was calculated based on equation (4).

$$\frac{H_2}{CO} = \frac{F_{H_2}}{F_{CO}} \quad (4)$$

3. RESULTS AND DISCUSSION

3.1 Characterization of the Catalysts

Figure 1 shows the low- and wide-angle XRD patterns of SBA-15 and Ni/SBA-15 catalysts prepared by different Ni-loading methods.

As shown in Figure 1(A), all the catalysts showed three peaks at $2\theta = 0.9, 1.6$ and 1.8° , corresponding to the (100), (110) and (200) which are reflections of typical two dimensional, hexagonally ordered mesostructures ($p6mm$), demonstrating the high quality of the mesopores packing [10]. The introduction of Ni has decreased the intensity of the peaks, suggesting partial blocking of the mesoporous structure. The changes in the XRD peaks are more clearly seen by calculating the percentage crystallinity of catalyst as

listed in Table 1. By comparing the effects of Ni-loading methods, it was observed that the percentage crystallinity followed the order of Ni/SBA-15(IE) > Ni/SBA-15(IM) > Ni/SBA-15(PM) indicating physical mixing method results in serious aggregation of Ni particles on the surface of SBA-15, resulting the higher blocking of the mesoporous structure.

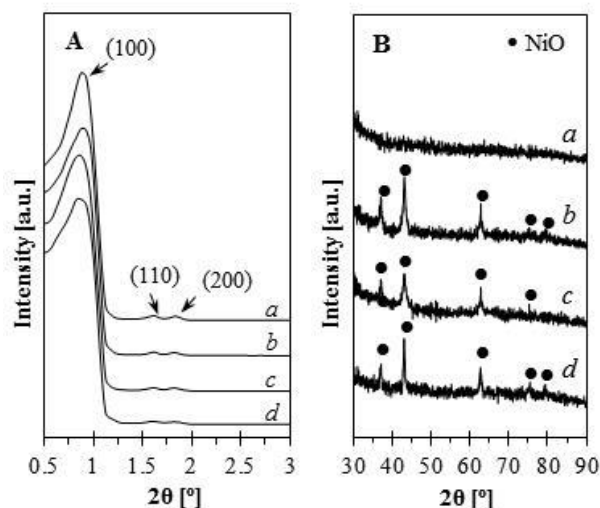


Fig. 1 (A) Low and (B) wide angle XRD patterns of (a) SBA-15, (b) Ni/SBA-15(IM), (c) Ni/SBA-15(IE) and (d) Ni/SBA-15(PM).

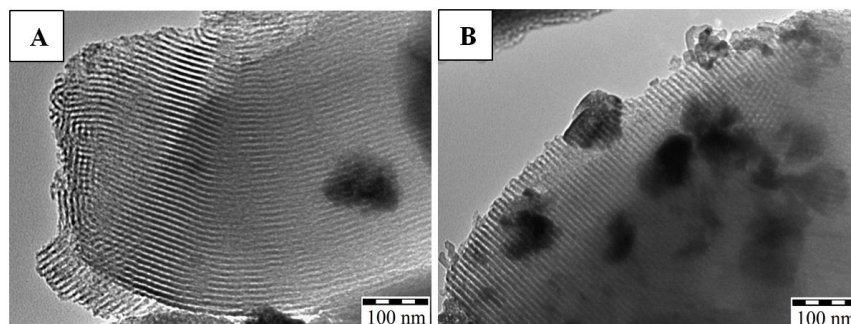


Fig. 2 TEM images of (A) Ni/SBA-15(IM) and (B) Ni/SBA-15(PM).

The BET surface area and pore volume of the SBA-15 and Ni/SBA-15 catalysts are shown in Table 1. It was observed that the introduction of Ni by impregnation, ion exchange and physical mixing had decreased the surface area and pore volume of the catalysts from 856 m²/g to 473, 594 and 426 m²/g, and from 0.999 cm³/g to 0.649, 0.623 and

0.469 cm³/g, respectively, indicating the blockage of the pores with Ni species. The presence of Ni on the surface of SBA-15 was characterized using wide-angle XRD analysis and the result shown in Figure 1(B). The XRD patterns of Ni/SBA-15 catalysts showed several diffraction peaks for NiO at 37.3°, 43.2°, 62.9°, 75.4° and 79.3° [4]. A measurement of the NiO crystallite size was carried out using scherrer equation at 2θ = 43.2° and the results are shown in Table 1. As shown in Table 1, it was observed that NiO particle sizes followed the order of Ni/SBA-15(IE) < Ni/SBA-15(IM) < Ni/SBA-15(PM) indicating higher agglomeration degree of Ni/SBA-15(PM) which might due to the weaker metal-support interaction presence in the catalyst. Several research groups were also reported higher agglomeration degree of metal due to the weaker metal-support interaction including Ni/MSN(PM) [4] and Co/SiO₂ [12] catalysts.

The higher agglomeration degree of Ni/SBA-15(PM) was confirmed by comparing the TEM images of Ni/SBA-15(IM) and Ni/SBA-15(PM) as shown in Figure 2, in which the presences of the Ni particles were observed by the occurrence of the spots with darker contrast areas. It was observed that the Ni/SBA-15(PM) catalyst has serious agglomeration as compared to the Ni/SBA-15(IM) catalyst. The result observed in TEM analysis was in agreement with the XRD analysis.

0.469 cm³/g, respectively, indicating the blockage of the pores with Ni species.

The blockages of SBA-15 pores with the introduction of Ni species were also reported on the Ni/SBA-15 prepared by P123-assisted method [1] and heat treatment method [9].

Table 1 Physical properties of SBA-15, Ni/SBA-15(IM), Ni/SBA-15(IE) and Ni/SBA-15(PM).

Catalyst	XRD crystallinity (%)	BET Surface Area (m ² /g)	Pore volume (cm ³ /g)	Ni particle size (nm) ^a
SBA-15	100	856	0.999	-
Ni/SBA-15(IM)	91.3	473	0.649	13.6
Ni/SBA-15(IE)	94.8	594	0.623	11.6
Ni/SBA-15(PM)	89.6	426	0.469	18.5

^a Determine by XRD (Scherrer equation)

Figure 3 shows the FTIR spectra of KBr in the range of 1400 – 500 cm^{-1} and 3800 – 2500 cm^{-1} . For FTIR spectra in range of 1400 – 500 cm^{-1} (Figure 3(A)), there are four significant peaks observed at 1060, 961, 801 and 510 cm^{-1} , which are assigned to the asymmetric stretching Si-O-Si, Si-O stretching of Si-OH groups, symmetric stretching Si-O-Si, and tetrahedral bending of Si-O-Si, respectively [13-14]. The introduction of Ni by all three methods did not alter the intensities of the peaks at 1060, 801 and 510 cm^{-1} indicating neither asymmetric stretching Si-O-Si, symmetric stretching Si-O-Si nor tetrahedral bending of Si-O-Si interacted with Ni particles. However, the intensity of the peak at 961 cm^{-1} which was assigned to Si-O stretching of Si-OH had decreased slightly and became enveloped in the peak of 1060 cm^{-1} indicating the interaction of Ni particles with support by replacing the Si-OH with Si-O-Ni. Moreover, it was observed (inset figure) that the decrease in the intensity of the peak followed the order of Ni/SBA-15(IE) > Ni/SBA-15(IM) > Ni/SBA-15(PM) indicating that Ni/SBA-15(IE) had higher metal-support interaction as compared to other methods. The direct evidence for the formation of Si-O-Ni by substitution of O-H with O-Ni was observed in Figure 3(B). The intensity of the peak at 3400 cm^{-1} which was assigned to O-H stretching vibration mode of Si-OH involved in hydrogen interaction with the adsorbed water molecules was decreased with the order of Ni/SBA-15(IE) > Ni/SBA-15(IM) > Ni/SBA-15(PM) due to the substitution of O-H with O-Ni.

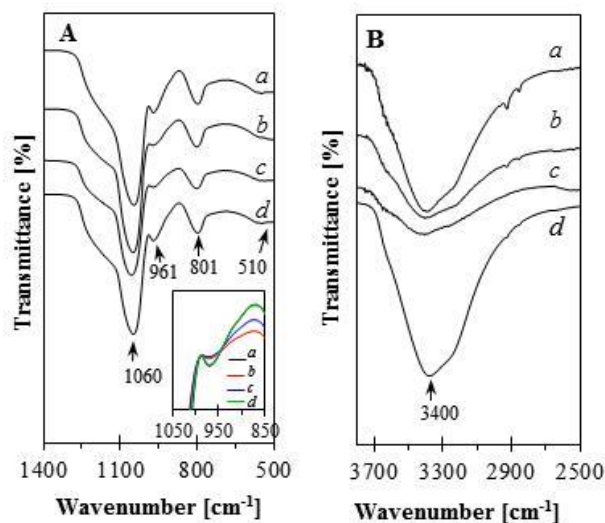


Fig. 3 FTIR spectra of KBr in the range of (A) 1400 – 500 cm^{-1} and (B) 3800 – 2500 cm^{-1} of (a) SBA-15, (b) Ni/SBA-15(IM), (c) Ni/SBA-15(IE) and (d) Ni/SBA-15(PM).

The change of the FTIR peaks caused by the introduction of metal was also observed on Cu and Cr supported SBA-15 reported by Tsoncheva et al. [15]. They found that the introduction of Cu and Cr resulted in slight red shift of the peak at 965 cm^{-1} indicating the partial metal incorporation and the formation of O-M (M is Cu(II) or

Cr(VI) type linkage. In addition, Xia et al. [16] reported that the introduction of Co into the SBA-15 decreased the absorbance intensity of nonbridging oxygen atoms ($\text{Si-O}^{\delta-}$) of Si-OH stretch at 970 cm^{-1} implying that Si-OH groups were consumed and transformed to Si-O-Co bonds. On the basis of the literature, thus, it is reasonable to conclude that the decreased of the peak at 961 cm^{-1} was related with the formation of Ni-support interaction (Si-O-Ni) through the substitution of O-H with O-Ni.

Figure 4 shows the TGA curves of SBA-15 and Ni/SBA-15 catalysts prepared by different Ni-loading methods. All the catalysts showed a weight loss region in the range of 27 °C to 200 °C, indicating the loss of catalyst water content. It was observed that the introduction of Ni on SBA-15 had reduced the amount of weight loss, that might be due to the elimination of hydrogen interaction between silanols and adsorbed water molecules by the substitution of surface silanol groups with Ni species. With regards to the effects of preparation methods, the weight loss of catalysts was following the order of Ni/SBA-15(PM) > Ni/SBA-15(IM) > Ni/SBA-15(IE) indicating that Ni/SBA-15(IE) had the lowest amount of water content due to the higher amount of metal-support interaction (Si-O-Ni).

The trend observed in TGA analysis was in agreement with the FTIR analysis. A decrease in the weight loss percentage caused by the removal of OH groups through the interaction of metal with support was also observed on the Ir-HZSM5 in which the mass loss region in the range of 25 to 350 °C was less pronounced when the HZSM-5 contains Iridium [17].

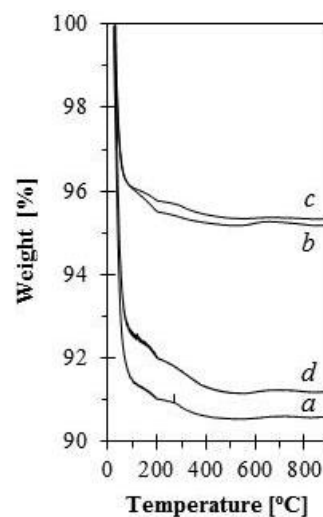


Fig. 4 TGA curves of (a) SBA-15, (b) Ni/SBA-15(IM), (c) Ni/SBA-15(IE) and (d) Ni/SBA-15(PM).

3.2. Catalytic Testing

Figure 5(A) and 5(B) show the conversion of CH_4 and CO_2 of SBA-15 and Ni/SBA-15 prepared by different Ni-loading methods at 800 °C. The reaction of SBA-15

showed lower activity (< 5 %) indicating that Ni particles are necessary for the studied catalytic reaction. The effects of Ni-loading methods are more clearly seen by calculating the average conversion and average H₂/CO ratio for 10 h of reaction as shown in Figure 5(C).

At temperature studied, the activity of catalysts followed the order of Ni/SBA-15(IE) \approx Ni/SBA-15(IM) > Ni/SBA-15(PM), while the stability and H₂/CO ratio followed the order of Ni/SBA-15(IE) > Ni/SBA-15(IM) > Ni/SBA-15(PM). The lowest activity of Ni/SBA-15(PM)

might be related to the larger Ni particles size arose from the weaker Ni-support interaction, where the Ni particles of PM method were preferentially agglomerate and decorating the surface part of SBA-15. Thus, it is believed that the Ni/SBA-15 that has higher Ni-support interaction are responsible for the best catalytic performance with high stability, while, Ni/SBA-15 that has weaker Ni-support interaction results in the higher agglomeration of Ni particles and thus resulted in lower performance and stability.

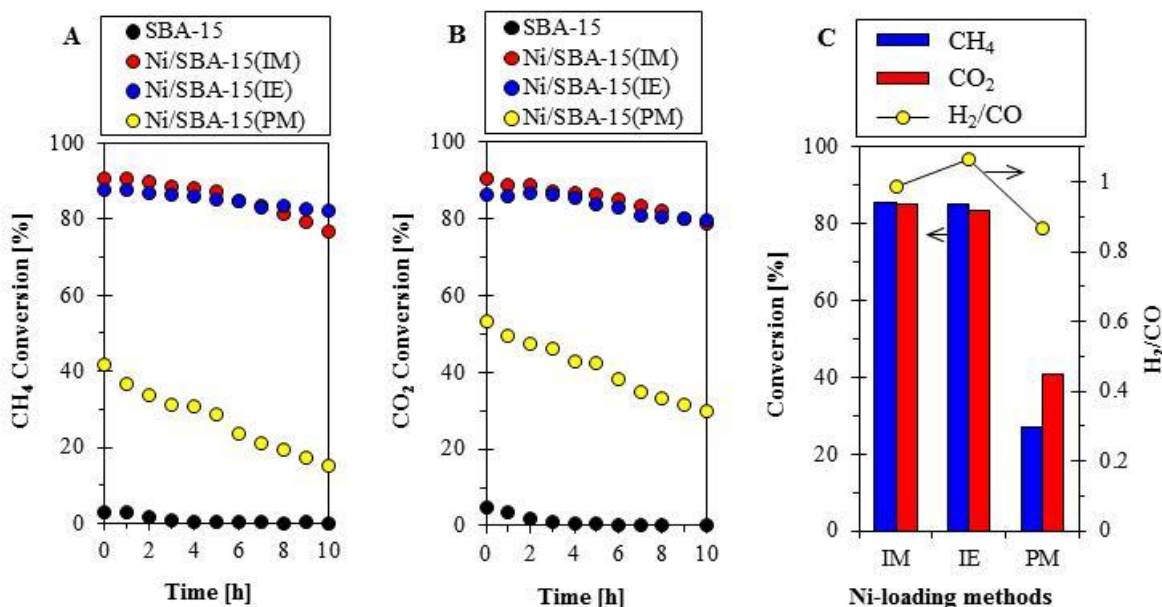


Fig. 5 (A) CH₄ conversion and (B) CO₂ conversion of SBA-15, 3Ni/SBA-15, 5Ni/SBA-15 and 10Ni/SBA-15 in CO₂ reforming of CH₄. (C) Effect of Ni-loading methods on the CH₄ conversion, CO₂ conversion and H₂/CO ratio.

The relationship between metal support interaction and catalytic activity of the catalyst was also observed on the Ni/MSN catalyst as reported by Sidik et al. [4]. They found that the Ni/MSN prepared by in-situ method has the highest catalytic activity as compared to impregnation and physical mixing methods due to the formation of strong metal support interaction (Si-O-Ni) through sequential desalination-substitution during the catalyst preparation. According to the proposed mechanism for CO₂ reforming of CH₄, the stepwise adsorption of CH₄ follows by its decomposition into CH_x fragments occurs on active metal sites, whereas CO₂ activation occurs mainly over the support. Thus, they claimed that the excellent catalytic activity is closely related to the availability of a great number of exposed Ni sites arose from the existence of strong metal support interaction (Si-O-Ni) which improved the dispersion of Ni active sites. In addition, Jing et al. [18] studied the influence of metal support interaction on the catalytic performance of Ni/SrO-SiO₂. They found that the structure of the Ni active phase was strongly depended on the interaction between Ni and the support, which related to the preparation methods. Based on the results obtained, they claimed that the enhanced

interaction between Ni species and SrO-SiO₂ might be responsible for the high activity of the catalyst towards the reformation of CH₄ with CO₂ and O₂. Therefore, on the basis of literature and the results obtained in this study, it is reasonable to conclude that the Ni-support interaction is responsible for an excellent catalytic performance and high stability of Ni/SBA-15 catalyst for CO₂ reforming of CH₄.

4. CONCLUSION

In this study, a series of Ni/SBA-15 catalysts were prepared with three different methods which were impregnation (IM), ion exchange (IE) and physical mixing (PM). The results showed that the different Ni-loading methods influence the properties and catalytic performance of Ni/SBA-15 towards CO₂ reforming of CH₄. The characterization analyses showed that the quantity of metal support interaction followed the order of Ni/SBA-15(IE) > Ni/SBA-15(IM) > Ni/SBA-15(PM), while the size of Ni particles, an agglomeration of Ni particles and blockage of the pores increased with the order of Ni/SBA-15(IE) < Ni/SBA-15(IM) < Ni/SBA-15(PM). At temperature studied,

the activity of catalysts followed the order of Ni/SBA-15(IE) \approx Ni/SBA-15(IM) > Ni/SBA-15(PM), while the stability of catalysts followed the order of Ni/SBA-15(IE) > Ni/SBA-15(IM) > Ni/SBA-15(PM). It was found that the introduction of Ni by IE resulted to the higher catalytic performance and stability, owing to the higher formation of Ni-support interaction by substitution of the Si-OH with Si-O-Ni. Meanwhile, the introduction of Ni by PM resulted to lower catalytic performance due to the higher agglomeration of Ni particles that were decorating on the surface part of SBA-15 arose from the weaker Ni-support interaction.

ACKNOWLEDGEMENTS

The authors are grateful for the financial support from Ministry of Education Malaysia through Research Acculturation Grant Scheme (RDU 151414) and Universiti Malaysia Pahang through Research University Grant (RDU140398).

REFERENCES

- [1] W. Yang, H. Liu, Y. Li, H. Wu, D. He, *Int. J. Hydrogen Energy* 41 (2016) 1513.
- [2] H. Liu, Y. Li, H. Wu, J. Liu, D. He, *Chin. J. Catal.* 36 (2015) 283.
- [3] D. Pakhare, J. Spivey, *Chem. Soc. Rev.* 43 (2014) 7813.
- [4] S.M. Sidik, S. Triwahyono, A.A. Jalil, M.A.A. Aziz, N.A.A. Fatah, L. P. Teh, *J. CO₂ Util.* 13 (2016) 71.
- [5] Y. Vafaeian, M. Haghighi, S. Aghamohammadi, *Energy Convers. Manage.* 76 (2013) 1093.
- [6] Y. Zhang, X. Zhu, D. Mei, B. Ashford, X. Tu, *Catal. Today* 256 (2015) 80.
- [7] X. Zhang, Q. Zhang, N. Tsubaki, Y. Tan, Y. Han, *Fuel* 147 (2015) 243.
- [8] L. Yao, J. Shi, H. Xu, W. Shen, C. Hu, *Fuel Process. Technol.* 144 (2016) 1.
- [9] B. Lu, K. Kawamoto, *Fuel* 103 (2013) 699.
- [10] D. Zhao, J. Feng, Q. Huo, N. Melosh, G.H. Fredrickson, B.F. Chmelka, G.D. Stucky, *Science* 279 (1998) 548.
- [11] B.D. Cullity, *Elements of X-ray Diffraction*, Second Edition., Addison-Wesley, Reading, MA, 1978.
- [12] Y. Zhang, Y. Liu, G. Yang, S. Sun, N. Tsubaki, *Appl Catal A*, 321 (2007) 79.
- [13] H. Jian, M. Renxiong, G. Zhihua, S. Chaofeng, H. Wei, *Chin. J. Catal.* 33 (2012) 637.
- [14] N. Brodie-Linder, S. Le Caër, M.S. Alam, J.P. Renault, C. Alba-Simionesco, *Phys. Chem. Chem. Phys.* 12 (2010) 14188.
- [15] T. Tsoncheva, M. Järn. D. Paneva, M. Dimitrov, I. Mitov, *Micropor. Mesopor. Mat.* 137 (2011) 56.
- [16] F. Xia, E. Ou, L. Wang, J. Wang, *Dye Pigments* 76 (2008) 76.
- [17] H.D. Setiabudi, S. Triwahyono, A.A. Jalil, N.H.N. Kamarudin, M.A.A. Aziz, *J. Nat. Gas Chem.* 20 (2011) 477.
- [18] Q. Jing, H. Lou, J. Fei, Z. Hou, X. Zheng, *Int. J. Hydrogen Energy* 29 (2004) 1245.